Journal of Research in Pharmacy

Research Article

www.jrespharm.com

Biophysical and thermodynamical insights into the interaction of mefenamic acid with human serum albumin, based on combined multi-spectroscopic and molecular modeling approaches

Golnaz PARVIZIFARD[1], Mostafa ZAKARIAZADEH[2], Hossein HAGHAEI[3], Mina SHABAN[4], Somaieh SOLTANI[5*]

[1] Department of Analytical Chemistry, Faculty of Chemistry, University of Tabriz, Tabriz, Iran
[2] Department of Biochemistry, Faculty of Sciences, Payame Noor University, Tehran, Iran
[3] Nutrition and Food sciences Faculty, Tabriz University of Medical Sciences, Tabriz, Iran
[4] Nanotechnology Research Center, Pharmaceutical Technology Institute, Mashhad University of Medical Sciences, and Mashhad, Iran
[5] Drug Applied Research Center and Pharmacy Faculty, Tabriz University of Medical Sciences, Tabriz, Iran
* Corresponding Author. E-mail: soltanis@tbzmed.ac.ir, Tel. +984133372254.

Received: 19 April 2023 / Revised: 28 June 2023 / Accepted: 01 July 2023

ABSTRACT: The molecular mechanism of interaction between Mefenamic acid (MA) and human serum albumin (HSA) was investigated. UV-Visible absorption, fluorescence, and FT-IR spectroscopies, with molecular docking, have been used for assay of complex formation, quenching mechanism study, thermodynamic evaluations, and molecular details of the interaction mechanism. The quenching constant (K_{sv}) of 1.51×10^5 M^{-1} was obtained, while the results are indicating the dynamic quenching mechanism. The number of binding sites (n) and apparent binding constants (KA) were 1.51 and 6.55×10^7 M^{-1}, respectively that resembles positive cooperativity and and strong binding of MA to HSA. The negative sign of standard enthalpy change (ΔH = -88.51 KJ/mol), standard entropy change (ΔS = -146.24 J/mol K), and Gibbs free energy (ΔG = -44.93 KJ/mol) indicated that the van der Waals interactions and hydrogen bonds are facilitating the MA-HSA complex formation. Addition of the metal ions, glucose, urea, and basic pHs decrease the MA-HSA binding constant. Molecular docking simulation showed that mainly positively charged amino acid residues contribute to the MA-HSA interaction.

KEYWORDS: Mefenamic acid, NSAID-HSA interaction, Spectroscopy methods, Molecular docking.

1. INTRODUCTION

The main protein that exists in the plasma, intracellular and interstitial fluids is human serum albumin (HSA). Its half-life is 19 days, and it plays a pivotal role as a reservoir and carrier protein in the blood. HSA structure and function studied well and findings revealed that the molecular roots of its extraordinary reversible ligand binding and delivering capacity [1]. The HSA molecular weight is 66.5 kD and it is consisting of one polypeptide chain. 585 amino acids with approximate dimensions of $80\times80\times30$ $Å^3$ composed the heart-shaped structure of HSA [2], that includes three homologous α-helical domains (I, II, and III). Two principal ligand binding sites are well known as Sudlow's site I (IIA) and Sudlow's site II (IIIA) [3-6]]. Zsila introduced the subdomain IB as a third main high-efficiency drug binding site in the HSA structure [7].
The pharmacological efficiency of a drug is closely related to its free concentration at the target site. Free concentration, distribution, biological activity, and the metabolism rate of drugs are influenced by their HSA binding [8, 9]. Structure HSA-binding relationship evaluations provide useful information for drug design and discovery, pharmacokinetics, and drug-drug interaction studies. Real-time and sensitive methods have developed using various spectroscopic techniques for drug-HSA interaction studies [10].

We reported the molecular mechanism of lamotrigine and carvedilol interaction with HSA, previously [2, 5]. We applied the same procedure for the study of Mefenamic acid (MA) interaction with HSA in the current

How to cite this article: Parvizi Fard G, Zakariazadeh M, Haghaei H, Shaban M, Soltani S. Biophysical and thermodynamical insights into the interaction of Mefenamic acid with human serum albumin, based on combined multi-spectroscopic and molecular modeling approaches. J Res Pharm. 2024; 28(1): 372-384.

ISSN: 2630-6344

http://dx.doi.org/10.29228/jrp.703

research. MA is an anthranilic acid derivative that belongs to the nonsteroidal anti-inflammatory drugs (NSAIDs). These drugs are recognized for their anti-inflammatory, analgesic, and antipyretic effects [11]. Most of the NSAIDs such as ibuprofen, diclofenac, *etc* can bind well to the HSA [12, 13]. MA contains a carboxylic acid moiety indicated in Figure 1 that is ionizing in the physiological pH. MA and its metabolites tightly bind to the HSA. UV-Visible spectroscopy, fluorescence quenching spectroscopy, FTIR were used for the investigation of MA–HSA interaction. The mode of interaction between MA and HSA was investigated by molecular docking.

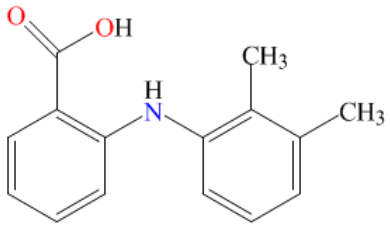

Figure 1. Chemical structure of MA.

2. RESULTS AND DISCUSSION

2.1. Fluorescence quenching titrations

Some parameter such as the excited-state reactions, complex-formation, energy transfer rate, and collisional quenching, resulting in the quenching of fluorescence emission [14]. Fluorescence quenching titration has been used for investigation of drug–HSA complex formation frequently [15, 16]. Fluorescence emission spectra of HSA (excited at 278 nm) and HSA-MA complex solutions are shown in Figure 2A. Trp214 as an intrinsic fluorophore is responsible for the fluorescence emission of HSA. The emission intensity of HSA (340 nm) decreased following the addition of enhanced concentrations of MA. The emission reduction confirms the MA-HSA coupling.

To identify the quenching mechanism (dynamic, static, or combined state), we fitted the obtained quenching data to the Stern–Volmer equation (Eq. 1).

$$F_0/F = 1 + K_{sv}[Q] \qquad \text{Eq. 1}$$

Where F_0 and F show the fluorescence intensities in the absence and presence of the quencher [Q]. K_{SV} is the Stern–Volmer quenching constant that shows the sensitivity of the fluorophore (Trp214) to the quencher (MA). Figure 2(B) shows the Stern-Volmer plot of MA-HSA interaction at 298K. The data fitted to a linear Stern-Volmer plot that indicates a static or dynamic mechanism of quenching. The resulted K_{SV} value (1.51×10^5 M^{-1}) indicated a strong quenching between MA and HSA was observed [17]. The obtained data for fluorescence quenching titrations at enhanced temperatures (298, 305, 310, and 315°K) were fitted to the Stern–Volmer equation and the results were presented in Figure 2(B) and Table 1. The enhanced K_{sv} values at higher temperatures suggested the dynamic quenching mechanism as the dominant mechanism in the MA - HSA interaction.

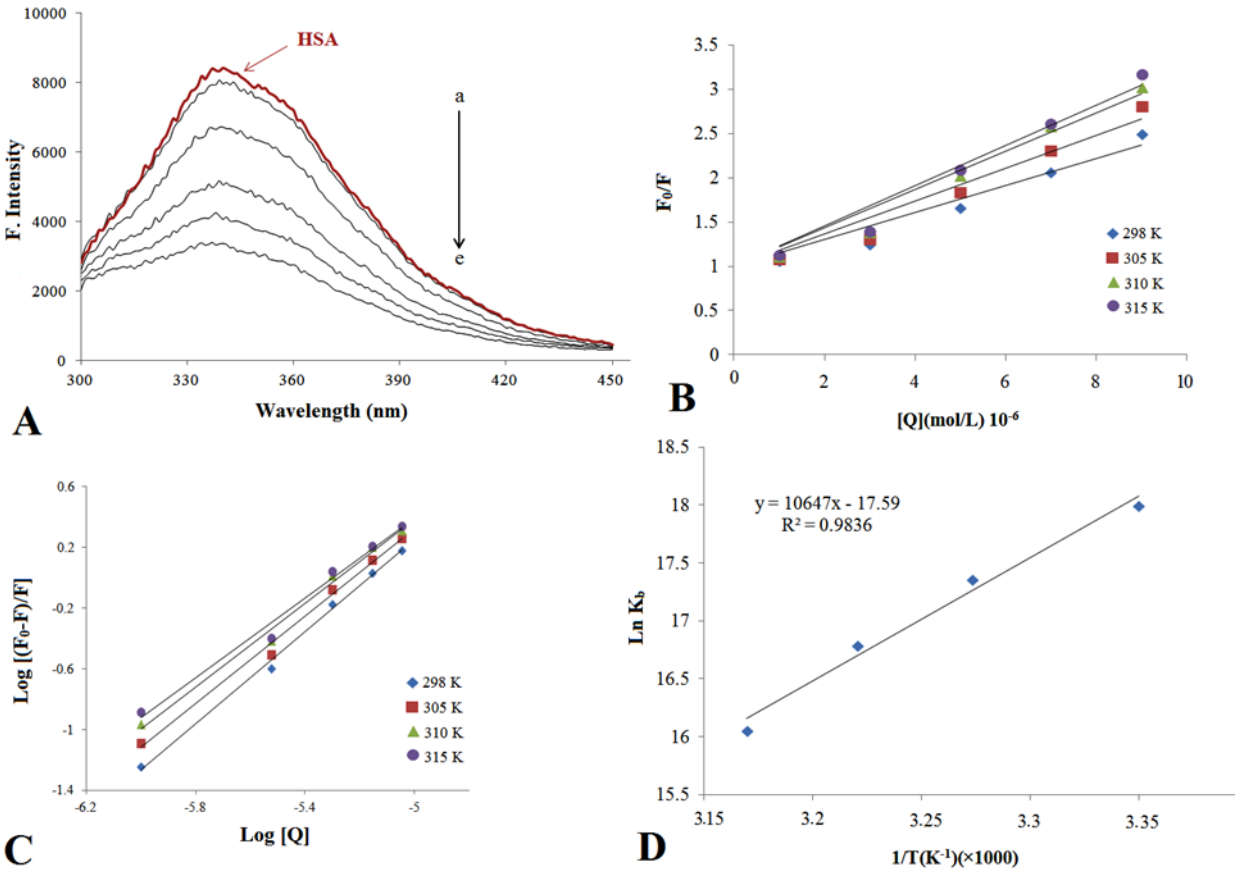

Figure 2. (A) Fluorescence spectra of HSA (7.5 µM) in the absence and presence of various amounts of MA (1-9 µM) at 298°K, (B) Stern-Volmer plot, (C) Hill plot, (D) Van't Hoff plot at 298-315°K.

Table 1. The Stern–Volmer quenching constant (Ksv), binding constant (Kb), binding site number (n), thermodynamic parameters of the interaction of HSA with MA at four different temperatures.

T (K)	Ksv (10^5 M^{-1})	$R_{SV\ plot}$	log K_A (M^{-1})	K_A (10^7 M^{-1})	n	$R_{Hill\ plot}$	lnK A	ΔH (KJ.mol^{-1})	ΔS (J.mol^{-1}K^{-1})	ΔG (KJ.mol^{-1})	R
298	1.51	0.97	7.81	6.55	1.51	0.99	18.00			-44.93	
305	1.85	0.97	7.53	3.44	1.44	0.99	17.35	-88.51	-146.24	-43.91	0.99
310	2.16	0.98	7. 29	1.95	1.38	0.99	16.78			-43.18	
315	2.27	0.98	6.97	0.93	1.31	0.98	16.05			-42.45	

2.2. Apparent binding constant and the number of binding sites

The binding constants (KA) and the binding cooperativity or number of the binding site (n) obtained using the Hill model (Eq. 2).

$$\log(F_0 - F)/F = log\ KA + n\ log\ [Q] \qquad \text{Eq. 2}$$

Where [Q] is the quencher concentrations (MA). Figure 2(C) shows the Hill plot of MA-HSA interaction at studied temperatures. KA and n values were presented in Table 1. KA at 298 K was 6.55×10^7 that confirms the strong interaction between MA and HSA. The reduction of KA at higher temperatures may result from HSA partial unfolding at higher temperatures. Binding cooperativity (n) of 1.51 at 298 K showed that there is a positive co-operativity between MA and HSA in which MA facilitates the binding of the second ligand to HSA after complex formation. The positive co-operativity was observed at all studied temperatures (Table 1), while n decreased due to the temperature enhancement. KA and n decreased due to the temperature enhancement (Table 1). This may occur due to the complex loosen at higher temperatures.

2.3. Mod of interaction between MA and HSA

The thermodynamic feature of MA-HSA complex formation was calculated using the fluorescence quenching titrations at enhanced temperatures (298, 305, 310, and 315°K). The data fitted to the van't Hoff equation (Eq. 3) for the calculation of entropy change (ΔS) and enthalpy changes (ΔH) [18]. Figure 2D shows the van't Hoff plot.

$$Ln\ KA = -\Delta H/RT + \Delta S/R \qquad \text{Eq. 3}$$

The constant of R is the gas constant value (8.314 J/mol×K) and T is the absolute temperature. Free energy changes (ΔG) were calculated using the Gibbs free energy (Eq. 4).

$$\Delta G = \Delta H - T\Delta S = -RT\ Ln\ KA \qquad \text{Eq. 4}$$

Obtained results are presented in Table 2. ΔH and ΔS values were -88.51 KJ.mol^{-1} and -146.24 J.mol^{-1}K^{-1}, respectively. Negative amounts for ΔH and ΔS shows the participation of the van der Waals and hydrogen bonding forces in the interaction due to the Ross and Subramanian [19]. The negative amount of ΔG (-44.93 KJ.mol^{-1} at 298K) indicates a feasible, spontaneous, and exothermal reaction between MA and HSA. ΔG values decreased by temperature enhancement (Table 2), which is a result of MA-HSA complex disassociation at higher temperatures.

Table 2. Calculated binding parameters of HSA-Mefenamic acid and HSA-site markers systems in the presence of two site indicators and MA-HSA interaction in acidic, neutral and basic pH.

System	K_{sv} (10^5 M^{-1})	K_A (10^5 M^{-1})	n		pH	Ksv (10^5 M^{-1})	K_A(10^7 M^{-1})	n
HSA-MA	1.85	655	1.51					
HSA-Warfarin	3.65	35.6	1.20		5.5	2.36	23.7	1.65
HSA-MA-Warfarin	1.78	9.31	1.14	**HSA-MA**	7.4	1.85	6.55	1.51
HSA-Ibuprofen	5.02	4.19	1.18		8	1.71	1.95	1.36
HSA- MA -Ibuprofen	0.62	0.93	1.04					

2.4. Determination of MA binding site in HSA by site markers

Warfarin and ibuprofen were used as subdomain IIA (Sudlow's site I) and subdomain IIIA (Sudlow's site II) site indicators [18]. The binding site I is a main binding site for heterocyclic anions and binding site II is selective for aromatic carboxylates [2]. MA binding site was determined using the site markers competitive substitute experiment at room temperature (25˚C). The fluorescence emission spectra of HSA and MA-HSA were obtained in the concentrations (1-9 µM) of each site marker. Figure 3(A, B) illustrated HSA fluorescence emission spectra with warfarin and ibuprofen, respectively. Figure 3(C, D) represents MA-HSA fluorescence emission spectra after the addition of warfarin and ibuprofen, respectively. The addition of site markers made a significant reduction of HSA and MA-HSA fluorescence intensities in the maximum emission wavelength.

A considerable, blue shift was observed by the addition of ibuprofen to the HSA-MA solutions that show the replacement of ibuprofen with MA (Figure 3(D)). A slight blue shift was also observed for the warfarin. The binding constant reduction in the presence of ibuprofen was significantly larger than warfarin (Table 1). The results revealed that MA interacts with the site IIIA with a higher tendency rather than the binding site IIA [20].

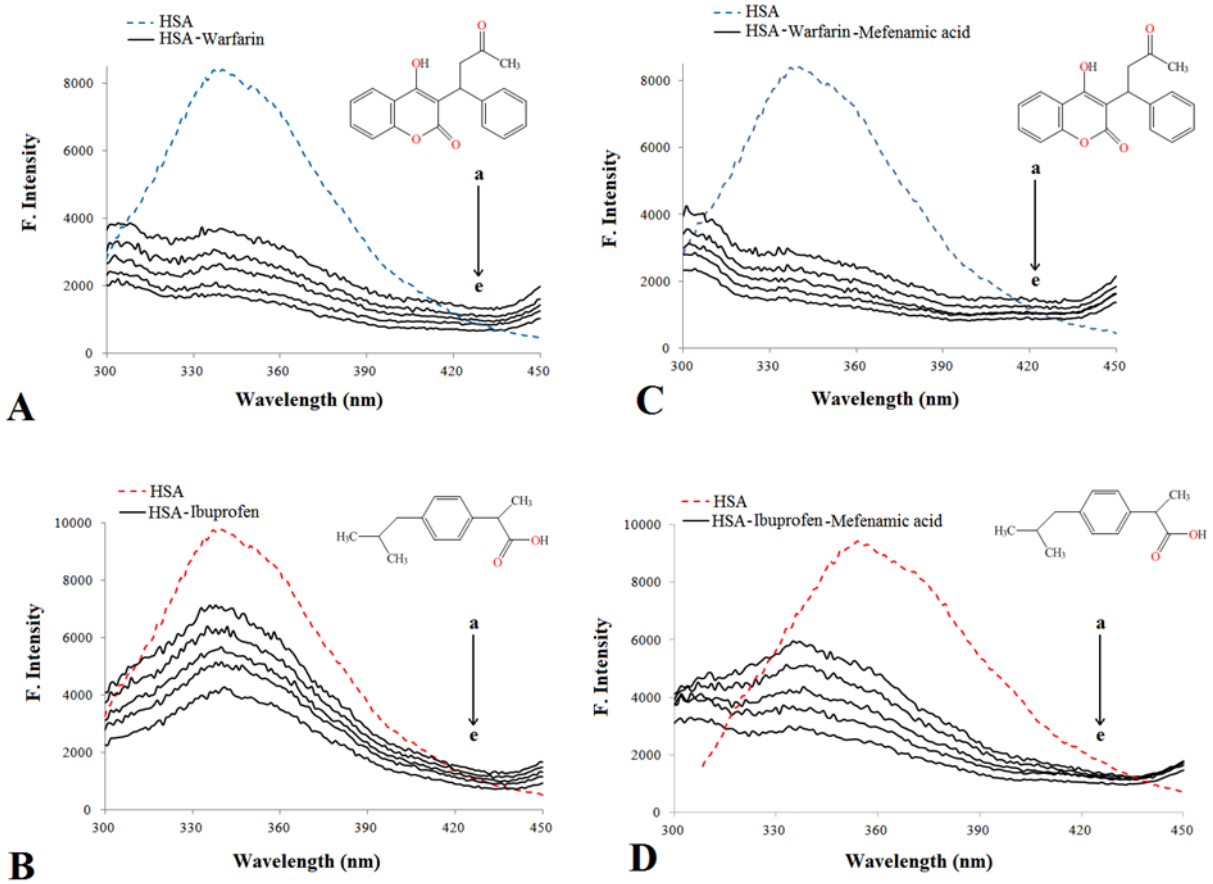

Figure 3. Fluorescence spectra of HSA in the presence of site indicators. Increased concentration of warfarin (A) and ibuprofen (B). Constant concentration of MA and increasing concentrations of warfarin (C) and ibuprofen (D).

2.5. MA-HSA interaction in acidic and basic pH

The ionization, solubility, stability, absorption, and other properties of acidic and basic drugs are influenced by pH [21]. Also, the HSA secondary structure alters due to the pH variation. HSA has four different conformational isomers/forms at pH <2.7 (extended (E)), pH 2.7-4.3 (fast-migrating (F)), pH 4.3-8.0 (neutral (N)), and pH>8.0 (basic (B)) [22]. To investigate the effect of pH variation on the conversion of MA-HSA interaction, we studied the fluorescence quenching titrations in acidic and basic pH (5.5 and 8.0). The KA and n obtained from Hill plot at each pH are given in Table 2. KA and n were reduced at basic pH while it increased at acidic pH.

As the pka of MA is 4.20 [23], the proportion of its ionized concentration that is calculated by Henderson–Hasselbalch equation (Eq. 5) increases at more basic pHs. At basic pH the ionization of imidazole and amino groups of HSA decreases which leads to the enhancement of the net negative charge of HSA. The isoelectric point of HSA is 4.7 [5]. These alterations in ligand and protein charges lead to the reduced interaction between them.

$$log\frac{[A^-]}{[HA]} = pH - pKa \qquad \text{Eq. 5}$$

Also, MA lipophilicity at basic pH (log D =2.21) is lower than at acidic pH (log D = 3.57), which could be a result of reduced MA-HSA binding at basic pH.

2.6. Influence of metal ions, glucose, and urea on the interaction of MA with HSA

Metallic ions participate in coordinate bond formation in the structure of some proteins [24, 25] and in the catalytic activity of enzymes [26]. Albumin binds to different metal ions including Mg(II), Ca(II), Co(II/III), Cu(I/II), and Zn(II) in the plasma [27-29]. The presence of ions may increase or decrease drug-protein binding [30, 31]. MA interaction with HSA was studied in the presence of Na^+, Mg^{2+}, Fe^{2+}, Zn^{2+}, Cu^{2+}, and Ni^{2+} cations. K_{sv}, KA, and n were calculated and the results are shown in Table 3. These calculated values are around 10^5 M^{-1}. KA values of MA-HSA significantly decreased in the presence of the studied ions (Table 3). Mg^{2+} cation possessed the highest effect in KA reduction. The decrease of KA means the storage time of MA may decrease and it can easily release from HSA in the presence of the studied cations [28].

Table 3. Calculated binding parameters of HSA-Mefenamic acid and HSA-site markers systems in the presence of two site indicators and MA.

Ions	Ksv (10^5 M^{-1})	K_A(10^5 M^{-1})	n
----	1.85	655	1.51
Zn^{2+}	7.01	3.54	0.94
Fe^{2+}	8.35	2.07	0.88
Cu^{2+}	1.14	1.69	1.03
Na^+	8.92	1.35	0.84
Ni^{2+}	3.39	0.91	0.89
Mg^{2+}	8.08	0.45	0.76

HSA is not a glycoprotein, while the N-terminal amino group (side chain) of positively charged residues (lysine and arginine) of HSA undergo spontaneous and non-enzymatic glycation in some diseases like severe diabetes [32, 33]. Lys199, Arg218, Lys281 (subdomain IIA residues), and Arg410, Arg428, Lys439 (subdomain IIIA residues) undergo glycosylation. This modification rigorously impacts HSA physiological functions. Also, glycated HSA can form intra and intermolecular cross-link between side chains of glycated amino acids and different proteins. Cross-link leads to aggregation and fibrillation of albumin. Glycosylation cause to transition HSA secondary structure from a-helical to b-sheet structure [32]. One of the common ways in response to the protein conformational transitions is the change in emission spectra of Trp214 in glycosylated HSA. The interaction of MA to glycated HSA was studied by fluorescence quenching titrations. KA and n were 0.37×10^5 M^{-1} and 0.80, respectively for MA-glycated HSA. The affinity of MA to glycated HSA was significantly decreased and negative cooperativity (n<1) was observed for MA-glycated HSA system.

Serum urea concentration increased in some pathophysiological conditions such as renal failure (uremia). Urea alters HSA folding from N (native) to I (intermediate), and D (denatured) states [34, 35]. The intermediate (I) conformation mostly is the result of domain III unfolding. We studied the MA-HSA interaction in the presence of urea (7.5 µM) using fluorescence quenching titrations. In the studied concentration, urea may stabilize the intermediate conformation of HSA rather than HSA denaturation. KA and n values of MA-HSA

system in the presence of urea were decreased (4.67×10^5 M^{-1} and 1.01). This reduction is a result of domain III unfolding where it is the main binding site of MA.

2.7. Complex formation study by UV-Visible spectra

The UV-Visible absorption experiment was performed for investigating the secondary conformation alteration of HSA in the presence of MA as well as MA-HSA complex formation. HSA absorption spectra include two absorption bands at the wavelengths near 210 nm and 278 nm. The absorption around 210 nm is related to the α-helix structure of HSA that is associated with the electronic transition ($n \rightarrow \pi^*$) of C=O functional groups in the polypeptide backbone of protein. The absorption band seen near 278 nm is the consequence of $\pi \rightarrow \pi^*$ transition of aromatic amino acids (Trp, Tyr, and Phe) [28]. The micro-environment change of aromatic amino acids leads to the change in the $\pi \rightarrow \pi^*$ transition and the consequent variation of the absorption band. The HSA absorption intensity enhancement following the interaction with MA confirms the complex formation between HSA and MA (Figure 4(A)). Also, a single redshift was observed from 278 nm to 285 nm due to the MA addition that indicates the MA-HSA complex formation and consequent changing of amino acid microenvironments. Subtraction of the absorption spectrum of HSA (curve a) and MA (curve b) from HSA–MA spectrum (curve c) in Figure (4B) resulted in two completely different spectra (curve d and curve e) that don't superpose completely to MA and HSA spectra. The obtained results were confirmed the MA-HSA complex formation [16].

2.8. Fluorescence resonance energy transfer (FRET)

The physical phenomenon of fluorescence resonance energy transfer (FRET), is an electrodynamic circumstance that accrues among a donor molecule in its excited state and an acceptor molecule in the ground state via two roots; radiative and non-radiative energy transfer mechanisms. Energy transfers non-radiatively from a donor chromophore to an accepter molecule nearby a dipole-dipole interaction [36]. Energy transfer efficiency from a donor to an accepter process occurs when a donor chromophore yield to the fluorescent light, the fluorescence emission spectrum of the donor, and absorbance spectrum of the acceptor gate has an overlap region and the distance from donor to acceptor is less than 8 nm [9].

FRET was applied for calculating the interval distance (r) of the donor (HSA) and acceptor (MA). R_0 as a critical distance when the transfer efficiency is 50% [5]. r was calculated using the method explained in our previous studies [5, 9, 37]. The spectral overlap of the donor emission and the acceptor absorption (J) obtained using Eq. 6.

$$J = \sum F(\lambda)\epsilon(\lambda)\lambda^4\Delta\lambda / \sum F(\lambda)\Delta\lambda \qquad \text{Eq. 6}$$

where F (λ) indicates the fluorescence intensity of the fluorescent donor of wavelength λ and ε (λ) is the molar absorption coefficient of the acceptor at wavelength λ. we considered $K_2 = 2/3$, N = 1.36 and Φ = 0.15 for HSA. The spectral overlap and calculated energy transfer parameters for MA-HSA complex were shown in Figure 5. The obtained interval distance (r = 3.78 nm) is between 0.5 R_0 - 1.5 R_0 and lower than 8 nm, which confirms the energy transfers from HSA to MA with high probability [31].

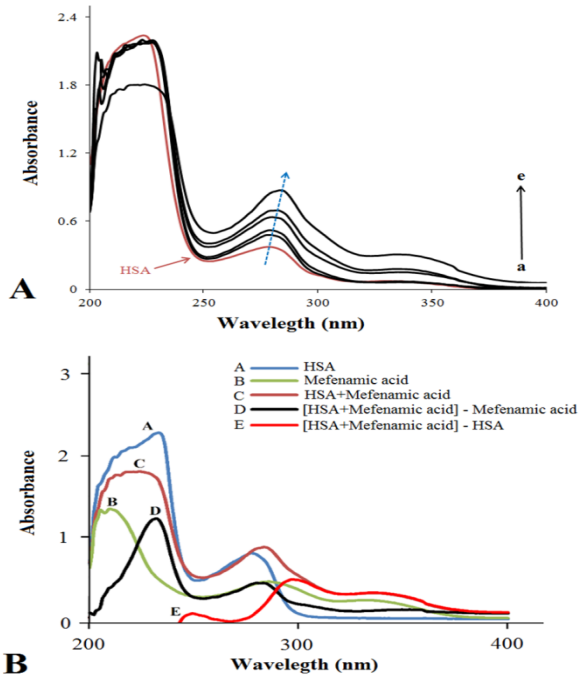

Figure 4. (A) UV-Visible absorption spectra of HSA in the presence of MA (a-e, 1-9 µM). Figure 4(B) Different absorption spectra of HSA-MA systems. (a) UV-Vis spectra of HSA, (b) MA, (c) HSA-Mefenamic acid system, (d) subtracting the absorption spectrum of HSA from HSA–MA system, and (e) subtracting the absorption spectrum of MA from HSA–MA system.

2.9. FT-IR spectra of the HSA and MA-HSA

The FT-IR spectra of free HSA (0.05 % (w/v)), pure MA, and MA-HSA were achieved in the range of 400–4000cm^{-1} at room temperature. The FT-IR spectra of HSA, MA, and MA–HSA complex were shown in Figure 6. The recorded FT-IR spectrum of free HSA shows the feature of amide I and amide II absorption bonds at 1650 and 1547 cm^{-1}, respectively (Figure6a). The peak position of C=O stretch and C=C in bonds of 1645 and 1404 cm^{-1} were shown in MA spectra. The bands at 1762, 1414, and 1018 cm^{-1} were assigned to C-N, C-H (aromatic hydrocarbon), and C-O stretch, respectively. Addition of MA to HSA resulted in the amide I and amide II bands' shift from 1650 cm^{-1} to 1637cm^{-1} and 1547 to 1535 cm^{-1}, respectively (Figure 6c). These shifts are contributed to the alteration of HSA secondary structure due to the MA binding [2, 38].

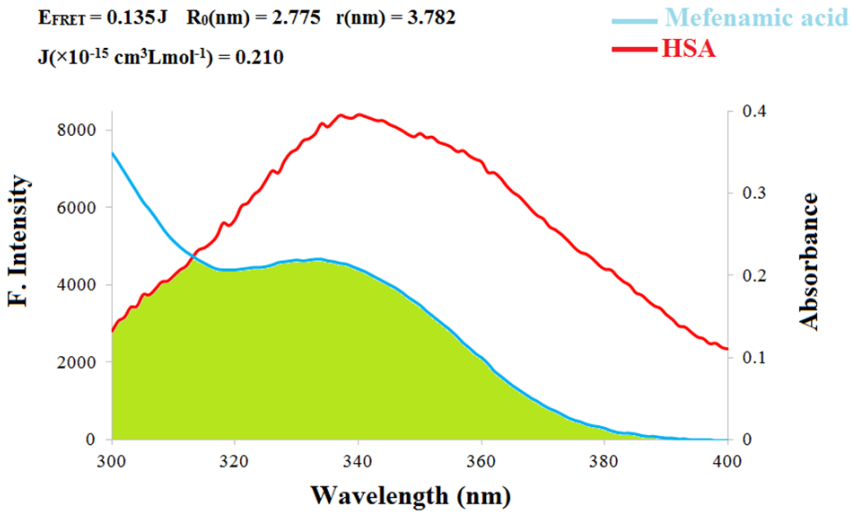

Figure 5. Overlapping between the fluorescence emission spectrum of HSA and absorption UV spectrum of MA (pH 7.4).

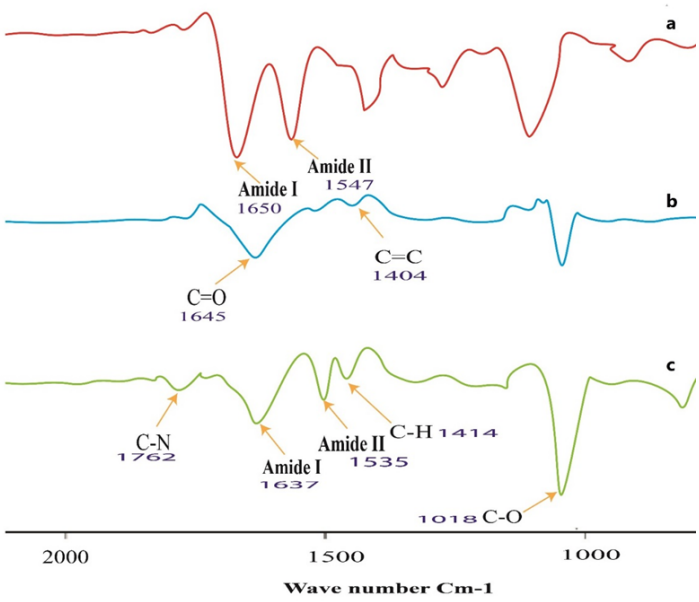

Figure 6. FT-IR spectra of different systems. (a) Free HSA, (b) pure MA, (c) complex HSA with MA.

2.10. Molecular docking results

MA docking to HSA shows the lowest free binding energy (ΔG= -9.53 Kcal/mol) in subdomain IIIA, which approves the site marker competition study and previous finding [7, 20]. MA also showed a high tendency to site IB (ΔG= -8.30 Kcal/mol). Another calculated free binding energy (ΔG) values for binding site IIA, IA, IIIB, and IIB are -7.18, -7.10, -7.01, and -5.96 Kcal/mol, respectively. Figure 7. A shows the lowest free binding energy conformer of MA docked to six different binding sites of HSA. The distance between the conformer with the lowest free binding energy (ΔG = -9.53 Kcal/mol) from Trp 214 is 0.98 nm (9.8 Å) (Figure 7.A), which is less than 8 nm and confirms the calculated approximate distance from FRET analysis (r =3.78nm). Polar amino acids mainly contribute to the MA–HSA binding (Table. 4). Positively charged Arg and Lys amino acids as well as Tyr amino acid participated in the formation of the hydrogen bonds via the carboxylic acid functional group of MA and mainly amino groups of HSA amino acids. Interactions between HSA binding site residues and MA presented by two-dimensional mode in Figure 7.B which was prepared by Lig Plot⁺ v 1.4.4 software [39]. These findings were confirmed the obtained experimental results that suggested hydrogen bonds as the main forces between HSA and MA.

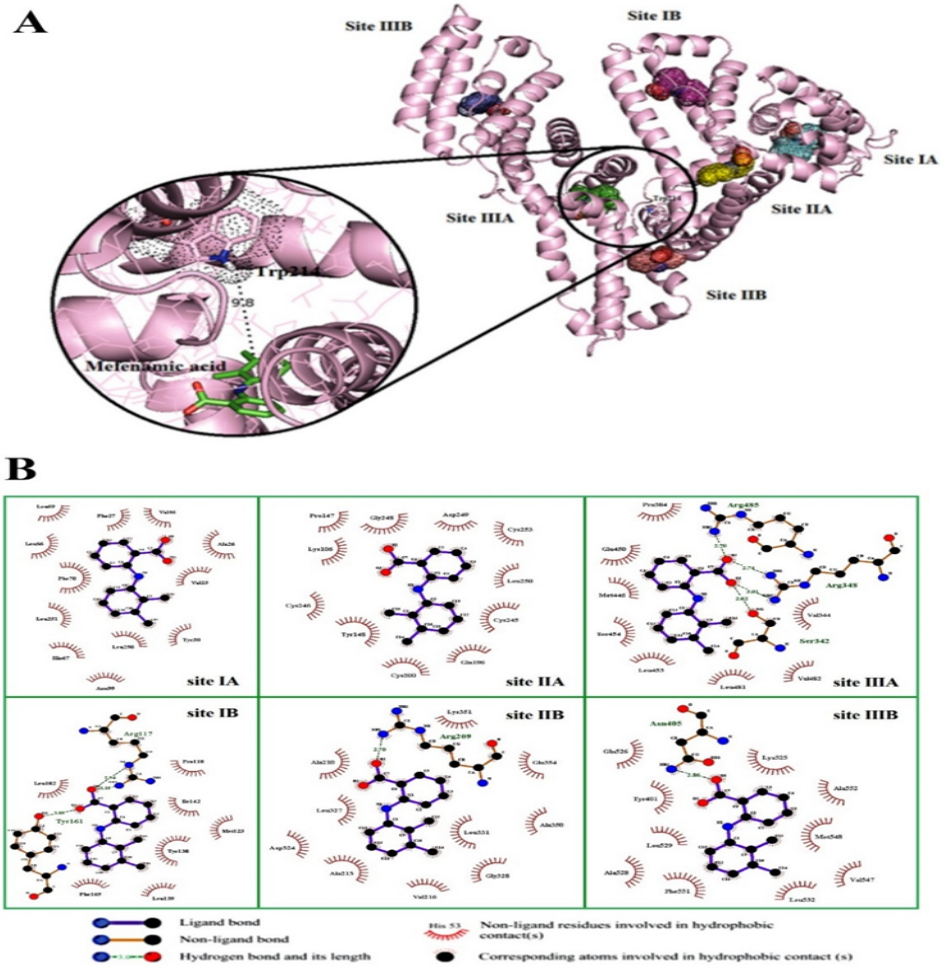

Figure 7. A. The lowest free binding energy conformers of MA docked to six different binding sites of HSA. Measured distance between Trp214 and MA is 9.8 Å and Figure 7.B. Interactions of MA and HSA in each binding site presented by two dimensionally mode.

Table 4. Amino acids of HSA that interacted and formed hydrogen bonds with Mefenamic acid. Amino acids in hydrogen bond formation are bolded.

Binding Site	I	II	III
A	Val23-Ala26-**Tyr30**-Val46-Leu66-His67-Leu69-Phe70-Asn99-Leu250-Leu251, **Lys73-Arg81-Glu82**	Lys106-Pro147-Tyr148-Tyr150-Gln196-Cys200-Cys245-Cys246-Gly248-Leu250-Cys253, **Ser202-Ser342-Arg348-Arg410-Tyr411-Lys414-Arg485**	Ser342-Val344-Arg348-Pro384-Met446-Ala449-Glu450-Leu453-Ser454-Leu481-Arg485, **Tyr148-Lys199-Arg218-His242**
B	**Arg117-**Pro118-Met123-Leu135-Tyr138-Leu139-Ile142-**Tyr161-**Phe165,	**Arg209**-Ala213-Val216-Asp324-Leu327-Gly328-Leu331-Ala350, **Lys378**	Tyr401-**Asn405**-Lys525-Ala528-Leu529-Leu532-Val547-Met548-Phe551-Ala552, **Lys525-Ser579**

3. CONCLUSION

The molecular mechanism of interaction between HSA and MA was investigated in this research. Some spectroscopic techniques and molecular docking simulations were used. The outcomes demonstrated that HSA fluorescence was quenched by MA through a dynamic mechanism. The binding constant and number of the binding site were 6.55×10^{7} M^{-1} and 1.51, respectively. This result indicated a strong interaction between HSA and MA and positively co-operative during the interaction. Negative signs of ΔH and ΔS suggest the

contribution of van der Waals interactions and hydrogen bonds as dominant forces in the binding of MA to HAS. The reaction is spontaneous and exothermal based on thermodynamic Gibbs free energy value. Site indicator experiment determined the interaction of MA with subdomain IIIA. Also, in the presence of metallic ions, glucose, and urea the number of binding constants was reduced. The appropriate distance between Trp-214 fluorophore and MA confirmed the probability of energy transfer. Docking results are in agreement with experimental findings. MA has a high binding tendency to ibuprofen site and the hydrogen bond paly a dominant role in the interaction. The reported results may increase the knowledge about the drug interaction with HSA and the contribution of endogenous chemicals such as metal ions, glucose, and urea on the interaction. Also, the results could be used in decision making for patients with diabetes, acidosis, alkalosis, and specific diets.

4. MATERIALS AND METHODS

4.1. Reagents

The Fatty acid HSA (>97% purity) was purchased from Sigma Aldrich. Methanol, KH_2PO_4, and NaOH were from the Merck Company. MA and ibuprofen were gifted by Sobhan Daru Company (Iran). Stock solutions of HSA (7.5×10^{-5} M, 0.5% w/v) were prepared daily by dissolving of 0.01g HSA in 2 mL of phosphate buffer (25 mM, pH 7.4). The main stock solution of MA (10^{-3} M) was obtained by disintegrating of 0.002g in 10 mL methanol and diluted with phosphate buffer to obtain working solutions (1×10^{-6}, 3×10^{-6}, 5×10^{-6}, 7×10^{-6}, 9×10^{-6} M). MA and HSA complex solutions were prepared by the dilution of enhanced concentrations of MA in the HSA solution.

4.2. Instruments

A double beam UV-Visible scanning spectrophotometer (UV-1800, Shimadzu, Japan) with a 1.0 cm quartz cell was used for the recording of UV spectra of studied solutions. The UV spectra were investigated in the range of 200–400 nm at 298 K with a scan rate of 250 nm min^{-1}.

The fluorescence quenching titrations were studied using a multi-mode reader Cytation™5, BioTek Instrument. The emission spectra of the studied solutions were obtained in the wavelength range of the 250-500 nm following the excitation at the wavelength of 278 nm. The FT-IR spectra (BRUKER, TENNSOR 27/37) with the range of 400–4000 cm^{-1} was used to recording analysis data.

4.3. Molecular docking study

To study the molecular interactions of MA with the HSA molecular docking method was performed [40]. The crystallographic structure of the HSA was acquired from the protein data bank. With 4Z69 PDBID Code (resolution = 2.19 Å). For the preparation of protein structure, the extra chemical structures were removed. The 3D chemical structure of MA was prepared using Hyperchem 8.0 software with MM+ and AM1 as a molecular mechanics and semi-empirical methods, respectively [41-43]. The molecular docking simulation was carried out by AutoDock 4.2.6 and the results were analyzed by AutoDock Tools 1.5.6 [44]. MA and HSA structures were prepared for docking by the addition of the polar hydrogen and Gasteiger and Kollman charges. The grid box dimension size at grid points in x×y×z directions was optimized to 66×66×66 $Å^3$ with 0.375 Å grid spacing [45]. The Lamarckian genetic algorithm method was employed for the docking procedure with 100 runs [44]. AutoDock Tools default values of energy evaluation, number of generations, and population size were set.

Acknowledgements: The authors would like to acknowledge from the faculty of pharmacy (Tabriz University of Medical Sciences) for providing partial financial support via grant number 52/8750 to this research.

Author contributions: Somaieh Soltani is the supervisor of this work. Golnaz Parvizi Fard has performed all experiments interpretation and Analysis of data, writing and Mostafa Zakariazadeh, Hossein Haghaei, Mina Shaban have contributed sufficiently to the scientific work.

Conflict of interest statement: There is no conflict of interest to be declared.

REFERENCES

[1] Zsila F. Circular dichroism spectroscopic detection of ligand binding induced subdomain IB specific structural adjustment of human serum albumin. J Phys Chem B. 2013; 117(37): 10798-10806. https://doi.org/10.1021/jp4067108
[2] Poureshghi F, Ghandforoushan P, Safarnejad A, Soltani S. Interaction of an antiepileptic drug, lamotrigine with human serum albumin (HSA): Application of spectroscopic techniques and molecular modeling methods. J Photochem Photobiol B: Biology. 2017; 166: 187-192. https://doi.org/10.1016/j.jphotobiol.2016.09.046.
[3] Fanali G, Masi A, Trezza V, Marino M, Fasona M, Ascenzi P. Human serum albumin: From bench to bedside. Mol Aspects Med. 2012; 33(3): 209-290. https://doi.org/10.1016/j.mam.2011.12.002
[4] Patra S, Santhosh K, Pabbathi A, Samanta A. Diffusion of organic dyes in bovine serum albumin solution studied by fluorescence correlation spectroscopy. RSC Advances. 2012; 2(14): 6079-6086. https://doi.org/10.1039/C2RA20633A.
[5] Safarnejad A, Shaghaghi M, Dehghan G, Soltani S. Binding of carvedilol to serum albumins investigated by multi-spectroscopic and molecular modeling methods. J Lumin. 2016; 176: 149-158. https://doi.org/10.1016/j.jlumin.2016.02.001
[6] Zhang J, Zhuang S, Tong C, Liu W. Probing the molecular interaction of triazole fungicides with human serum albumin by multispectroscopic techniques and molecular modeling. J Agric Food Chem. 2013; 61(30): 7203-7211. https://doi.org/10.1021/jf401095n
[7] Zsila F. Subdomain IB is the third major drug binding region of human serum albumin: toward the three-sites model. Mol Pharm. 2013; 10(5): 1668-1682. 10.1021/mp400027q
[8] Alam A, Uddin R, Haque S. Protein binding interaction of warfarin and acetaminophen in presence of arsenic and of the biological system. Bangladesh J Pharmacol. 2008; **3**(2): 49-54. 10.3329/bjp.v3i2.835
[9] Xu H, Yao N, Xu H, Wang T, Li G, Li Z. Characterization of the interaction between eupatorin and bovine serum albumin by spectroscopic and molecular modeling methods. Int J Mol Sci. 2013; 14(7): 14185-14203. 10.3390/ijms140714185
[10] Bojko B, Sutkowska A, Maciqzek-Jurczyk M, Rownicka J, Sulkowski W. Investigations of acetaminophen binding to bovine serum albumin in the presence of fatty acid: fluorescence and 1H NMR studies. J Mol Struct. 2009; 924: 332-337. https://doi.org/10.1016/j.molstruc.2008.12.015
[11] Bally M, Dendukuri N, Rich B, Nadeau L, Helin-Salmivaara A, Garbe E, Brophy J. Risk of acute myocardial infarction with NSAIDs in real world use: bayesian meta-analysis of individual patient data. BMJ. 2017; 357: j1909. https://doi.org/10.1136/bmj.j1909
[12] Bukkitgar S, Shetti N, Nayak D, Bagehalli G, Nadibewoor S. Electrochemical sensor for the detection of mefenamic acid in pharmaceutical sample and human urine at glassy carbon electrode. Der Pharma Chemica. 2014; 6(2): 258-268.
[13] Dhumal BS, Bhusari KP, Ghante MH, Jain NS. UV spectrophotometric analysis for the determination of mefenamic acid in pharmaceutical formulation. IAJPR. 2015. 5(11): 3643-3650. http://www.scopemed.org/?mno=211166.
[14] Lakowicz J. Principles of fluorescence spectroscopy (ed. Lakowicz, JR) 1–14. 2013, Springer Science & Business Media.
[15] Shahabadi N, Khorshidi A, Moghadam NH. Study on the interaction of the epilepsy drug, zonisamide with human serum albumin (HSA) by spectroscopic and molecular docking techniques. Spectrochim Acta A Mol Biomol Spectrosc. 2013; 114: 627-632. https://doi.org/10.1016/j.saa.2013.05.092.
[16] Tian, F, Li J, Jiang F, Han X, Xiang C, Ge Y, Li L, Liu Y. The adsorption of an anticancer hydrazone by protein: an unusual static quenching mechanism. RSC Advances. 2012; 2(2): 501-513. https://doi.org/10.1039/C1RA00521A.
[17] Ciepluch K, Katir N, Kadip AE, Weber M, Caminade AM, Bousmina M, Majoral JP, Bryszewska M. Photo-physical and structural interactions between viologen phosphorus-based dendrimers and human serum albumin. J Lumin. 2012; 132(6): 1553-1563. https://doi.org/10.1016/j.jlumin.2012.01.044
[18] Zhou N, Liang Y, Wang P. 18β-Glycyrrhetinic acid interaction with bovine serum albumin. J Photochem Photobiol A Chem 2007; 185(2-3): 271-276. https://doi.org/10.1016/j.jphotochem.2006.06.019
[19] Haghaei H, Hosseini SRA, Soltani S, Fathi F, Mokhtari F, Karima S, Rashidi M. Kinetic and thermodynamic study of beta-Boswellic acid interaction with Tau protein investigated by surface plasmon resonance and molecular modeling methods. Bioimpacts. 2020;10(1):17-25. https://doi.org/10.15171/bi.2020.03.
[20] Carter D, Ho J, Wang Z. Albumin binding sites for evaluating drug interactions and methods of evaluating or designing drugs based on their albumin binding properties. Google Patents, CA2585115A1.
[21] Taylor KM, Aulton ME. Aulton's Pharmaceutics E-Book: The Design and Manufacture of Medicines. Elsevier Health Sciences.2021.
[22] Ascenzi P, Fasano M. Allostery in a monomeric protein: The case of human serum albumin. Biophys Chem. 2010; 148(1-3): 16-22. https://doi.org/10.1016/j.bpc.2010.03.001
[23] Wishart DS, Feunang YD, Guo AC, Lo EJ, Marcu A, Grant JR, Sajed T, Johnson D, Li C, Sayeeda Z, Assempour N, Iynkkaran I, Liu Y, Maciejewski A, Gale N, Wilson A, Chin L, Cummings R, Le D, Pon A, Knox C, Wilson M. DrugBank 5.0: a major update to the DrugBank database for 2018. Nucleic Acids Res. 2018;46(D1):D1074-D1082. https://doi.org/10.1093/nar/gkx1037.
[24] Dokmanić I, Šikić M, Tomić S. Metals in proteins: correlation between the metal-ion type, coordination number and the amino-acid residues involved in the coordination. Acta Crystallogr D Biol Crystallogr. 2008. 64(3): 257-263. https://doi.org/10.1107/S090744490706595X

[25] Safo MK, Ahmed MH, Ghatge MS, Boyiri T. Hemoglobin–ligand binding: Understanding Hb function and allostery on atomic level. Biochim Biophys Acta Proteins Proteom. 2011; 1814(6): 797-809. https://doi.org/10.1016/j.bbapap.2011.02.013
[26] Bolattin MB, Nandibewoor ST, Joshi SD, Dixit SR, Chimatadar SA. Interaction between carisoprodol and bovine serum albumin and effect of β-cyclodextrin on binding: Insights from molecular docking and spectroscopic techniques. RSC Advances. 2016; **6**(68): 63463-63471. https://doi.org/10.1039/C6RA08063D
[27] Deng B, Wang Y, Zhu P, Xu X, Ning X. Study of the binding equilibrium between Zn (II) and HSA by capillary electrophoresis–inductively coupled plasma optical emission spectrometry. Anal Chim Acta. 2010; 683(1): 58-62. 10.1016/j.aca.2010.10.018
[28] Shen GF, Liu TT, Wang Q, Jiang M, Shi J. Spectroscopic and molecular docking studies of binding interaction of gefitinib, lapatinib and sunitinib with bovine serum albumin (BSA). J Photochem Photobiol Biology. 2015; 153: 380-390. https://doi.org/10.1016/j.jphotobiol.2015.10.023
[29] Śliwińska-Hill U, Wiglusz K. The interaction between human serum albumin and antidiabetic agent–exenatide: determination of the mechanism binding and effect on the protein conformation by fluorescence and circular dichroism techniques-Part I. J Biomol Struct Dyn. 2020; 38(8): 2267-2275. ttps://doi.org/10.1080/07391102.2019.1630007
[30] Byadagi K, Meti M, Nandibewoor S, Chimatadar S. Investigation of binding behaviour of procainamide hydrochloride with human serum albumin using synchronous, 3D fluorescence and circular dichroism. J Pharm Anal. 2017; **7**(2): 103-109. https://doi.org/10.1016/j.jpha.2016.07.004
[31] Cheng Z. Interaction of ergosterol with bovine serum albumin and human serum albumin by spectroscopic analysis. Mol Biol Rep. 2012; 39: 9493-9508. https://doi.org/10.1007/s11033-012-1814-6
[32] Awasthi S, Nambiappan S. Non-enzymatic glycation mediated structure–function changes in proteins: case of serum albumin. RSC Advances. 2016; 6(93): 90739-90753. https://doi.org/10.1039/C6RA08283A
[33] Otagiri M, Chuang V. Pharmaceutically important pre-and posttranslational modifications on human serum albumin. Biol Pharm Bull. 2009; 32(4): 527-534. https://doi.org/10.1248/bpb.32.527.
[34] Chatterjee T, Pal A, Dey Scharita, Chatterjee BK, Chakrabarti P. Interaction of virstatin with human serum albumin: Spectroscopic analysis and molecular modeling. PloS One. 2012; 7(5): e37468. https://doi.org/10.1371/journal.pone.0037468
[35] Rehman, MT, Shamsi H, Khan AU. Insight into the binding mechanism of imipenem to human serum albumin by spectroscopic and computational approaches. Mol Pharm. 2014; 11(6): 1785-1797. https://doi.org/10.1021/mp500116c
[36] Kandagal PB, Ashoka S, Seetharamappa J, Shaikh SMT, Jadegoud Y, Ijare OB. Study of the interaction of an anticancer drug with human and bovine serum albumin: Spectroscopic approach. J Pharm Biomed Anal. 2006; 41(2): 393-399. https://doi.org/10.1016/j.jpba.2005.11.037
[37] Karami K, Jamshidian N, Zakariazadeh M. Synthesis, characterization and molecular docking of new C, N-palladacycles containing pyridinium-derived ligands: DNA and BSA interaction studies and evaluation as anti-tumor agents. Appl Organomet Chem. 2019; 33(3): e4728. https://doi.org/10.1002/aoc.4728
[38] Mudalip SKA, Bakar MRA, Adam F, Jamal P. Structures and hydrogen bonding recognition of mefenamic acid form I crystals in mefenamic acid/ethanol solution. Int J Chem Eng Appl. 2013; 4(3): 124-128. https://doi.org/10.7763/IJCEA.2013.V4.277
[39] Gomes DE, Caruso ÍP, de Araujo GC, de Lourenço IO, de Melo FA, Cornélio ML, Fossey MA, de Souza FP. Experimental evidence and molecular modeling of the interaction between hRSV-NS1 and quercetin. Int J Biol Macromol. 2016;85:40-47. https://doi.org/10.1016/j.ijbiomac.2015.12.051.
[40] Morris GM, Lim-Wilby M. Molecular docking. Methods Mol Biol. 2008;443:365-382. https://doi.org/10.1007/978-1-59745-177-2_19
[41] Soltani S, Babaei H, Asadpour-Zeynali K, Jouyban A. Modeling vasorelaxant activity of some drugs/drug candidates using artificial neural networks. J Pharmacol Toxicol. 2007; 2: 411-426. https://doi.org/10.3923/jpt.2007.411.426
[42] Tatardar S, Jouyban A, Soltani S. QSAR analysis of cyclooxygenase inhibitors selectivity index (COX1/COX2): Application of SVM-RBF and MLR methods. Pharm Sci. 2015; 21(2): 86-93. http://dx.doi.org/10.15171/PS.2015.22
[43] Zakariazadeh M, Barzegar A, Soltani S, Aryaour H. Developing 2D-QSAR models for naphthyridine derivatives against HIV-1 integrase activity. Med Chem Res, 2015; 24: 2485-2504. https://doi.org/10.1007/s00044-014-1305-5
[44] Morris GM, Huey R, Lindstrom W, Sanner MF, Belew RK, Goodsell DS, Olson AJ. AutoDock4 and AutoDockTools4: Automated docking with selective receptor flexibility. J Comput Chem. 2009;30(16):2785-2791. https://doi.org/10.1002/jcc.21256
[45] Karami K, Rahimi M, Zakariazadeh M, Buyukgungor O. A novel silver (I) complex of α-keto phosphorus ylide: Synthesis, characterization, crystal structure, biomolecular interaction studies, molecular docking and in vitro cytotoxic evaluation. J Mol Structure. 2019; 1177: 430-443. https://doi.org/10.1016/j.molstruc.2018.09.063